Macroscopic Thermodynamics of Kinetic Gas Theory through Computer Simulation

Usman Siddiqui

***Abstract*—We use Python to simulate a simple linear 2D time-discontinuous microscopic model of kinetic gas theory in a circular container. The simulation is used to confirm macroscopic thermodynamic properties proposed by the ideal gas and Van der Waals equations of state. We use the results to verify that mean free path is inversely proportional to the number of particles and the diffusion coefficient is proportional to the square root of the equilibrium temperature.**

I. Introduction

A computer simulation can be a powerful tool in analysis of chaotic systems since the experiment can be repeated multiple times with a defined set of initial conditions. In this report, we develop a computer simulation of a simple model of kinetic gas theory to experimentally verify equations of state and investigate other thermodynamic relations. We extend our findings to derive the mathematical dependence between thermodynamic properties (e.g. number density) and macroscopic observables (e.g. mean free path, diffusion coefficient). Our results represent the formulation of macroscopic thermodynamics from a simulation of microscopic behaviour, providing a proof-of-concept for deriving equations of state for other types of matter (e.g. photon gases).

II. Theory

To improve efficiency, the particles move in linear motion between frames and each frame skips to the next collision. This reduces the time-complexity of the problem from $O(N^2)$ to $O(N)$ using a collision table. For balls confined to a circular container, there are two types of collisions: ball-to-ball (B2B) collisions and ball-to-wall (B2W) collisions. Refer to [1] for derivations of (1), (2), (3) and (4).

A. B2W Collision

Suppose $\boldsymbol{r}$ is the position of a ball relative to the centre of the container and $\boldsymbol{v}$ is its velocity. Then the ball will collide with the wall at time $t = t_1$ where t_1 is the smallest, positive root of

$$(\boldsymbol{v}\cdot\boldsymbol{v})t^2 + 2(\boldsymbol{r}\cdot\boldsymbol{v})t + (\boldsymbol{r}\cdot\boldsymbol{r}) = (R-a)^2, \tag{1}$$

given that R and a are the radii of the container and ball, respectively. The rebound velocity of the ball is

$$\boldsymbol{v'} = \boldsymbol{v} - \frac{2(\boldsymbol{r}\cdot\boldsymbol{v})}{(\boldsymbol{r}\cdot\boldsymbol{r})}\boldsymbol{r}. \tag{2}$$

Kinetic energy is conserved but momentum is not since the container is fixed in space. The total magnitude of the momentum is conserved for the system.

B. B2B Collision

Consider the time at which a ball, A, with position, $\boldsymbol{r_A}$, and velocity, $\boldsymbol{v_A}$, will collide with another ball, B, with position and velocity defined similarly. The time of collision between A and B is given by the smallest, positive root of

$$(\boldsymbol{\delta v}\cdot\boldsymbol{\delta v})t^2 + 2(\boldsymbol{\delta r}\cdot\boldsymbol{\delta v})t + (\boldsymbol{\delta r}\cdot\boldsymbol{\delta r}) = (a_A + a_B)^2 \tag{3}$$

where $\boldsymbol{\delta r} = \boldsymbol{r_B} - \boldsymbol{r_A}$, $\boldsymbol{\delta v} = \boldsymbol{v_B} - \boldsymbol{v_A}$ and a_A and a_B are the radii of the two balls. If their masses are m_A and m_B, the rebound velocities are

$$\begin{aligned}\boldsymbol{v'_A} &= \boldsymbol{v_A} + m_B\boldsymbol{q}\\ \boldsymbol{v'_B} &= \boldsymbol{v_B} - m_A\boldsymbol{q},\end{aligned} \tag{4}$$

where $\boldsymbol{q}$ is

$$\boldsymbol{q} = \frac{2(\boldsymbol{\delta r}\cdot\boldsymbol{\delta v})}{(m_A+m_B)(\boldsymbol{\delta r}\cdot\boldsymbol{\delta r})}\boldsymbol{\delta r}. \tag{5}$$

Both kinetic energy and momentum are conserved in this collision.

III. Testing

The simulation is tested to ensure that conservation laws are obeyed. An oblique B2B collision between two balls is simulated to ensure momentum is conserved (Fig. 1). Then the simulation is run with multiple balls to verify confinement (conservation of mass), conservation of kinetic energy (see Appendix) and conservation of total magnitude of momentum.

We define the equilibrium state such that each ball has undergone, on average, five B2B collisions so that there has been a significant redistribution of kinetic energy in the system. Balls are systematically arranged in a lattice with random velocities and the system is allowed to tend to equilibrium.

A histogram of the separation at equilibrium between each pair of balls in a system of $N = 250$ balls is shown in Fig. 2(a). For container radius $R = 200\,\mathrm{m}$, the mean separation is $\Delta r = (180 \pm 80)\,\mathrm{m}$ and the Gaussian is indicative of successful dispersion. A histogram of the radial distance, r, for each ball at equilibrium is shown in Fig. 2(b). At equilibrium, the rate of change of concentration is zero so the number of balls per unit area is constant. Since the area of each radial disk increases with r, balls are more likely to be located away from the centre. The concentration gradient at equilibrium is zero (Fig. 3).

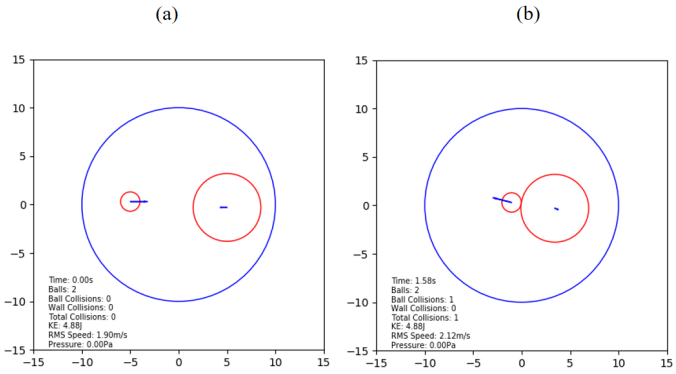

Fig. 1: A screenshot of the frames *(a)* prior to and *(b)* immediately after an oblique B2B collision. The blue arrows indicate velocity vectors of the balls. The mass of the smaller ball is $m_1 = 1.0\,\mathrm{kg}$ and its velocity is $(u_x, u_y) = (2.5, 0.0)\mathrm{m\,s^{-1}}$. The larger ball has mass $m_2 = 3.5\,\mathrm{kg}$ and velocity $(v_x, v_y) = (-1.0, 0.0)\mathrm{m\,s^{-1}}$. After the collision, the smaller ball is deflected with velocity $(u'_x, u'_y) = (-1.6, 2.3)\mathrm{m\,s^{-1}}$ and the larger ball is deflected with velocity $(v'_x, v'_y) = (0.17, -0.66)\mathrm{m\,s^{-1}}$. Momentum is conserved in this collision.

IV. Investigations

A. Rayleigh Distribution

The Maxwell-Boltzmann distribution is a fundamental result in kinetic gas theory which describes the *probability density* of a particle with speed v. It is a three-dimensional generalisation of the two-dimensional Rayleigh distribution [2]

$$f(v) = \frac{v}{b^2} \exp\left(-\frac{v^2}{2b^2}\right), \tag{6}$$

where

$$b^2 = \frac{kT}{m}, \tag{7}$$

is the Rayleigh parameter for particles of mass, m, at equilibrium temperature, T, and k is the Boltzmann constant. The Rayleigh distribution for v arises when components v_x and v_y are independently selected from a Gaussian distribution [1].

We use the simulation to reproduce the Rayleigh distribution. The initial state is configured with $N = 500$ balls, each with a randomly-oriented velocity of magnitude $\bar{v} = 10\,\mathrm{m\,s^{-1}}$. The system is allowed to reach equilibrium and the speed of each ball is plotted as a histogram (Fig. 4(a)). A value of $b^2 = (50 \pm 6)\,\mathrm{J\,kg^{-1}}$ is attained as a parameter estimate with coefficient of determination (COD) $R^2 = 0.98$ indicating a strong goodness-of-fit.

The experiment is repeated with the magnitude of the velocity set to $\bar{v} = 50\,\mathrm{m\,s^{-1}}$ and its corresponding histogram is shown in Fig. 4(b). The Rayleigh parameter is $b^2 = (5.0 \pm 0.6) \times 10^3\,\mathrm{J\,kg^{-1}}$ and has COD $R^2 = 0.91$ indicating an acceptable goodness-of-fit. By ideal gas theory, the equilibrium temperature is proportional to the mean-square

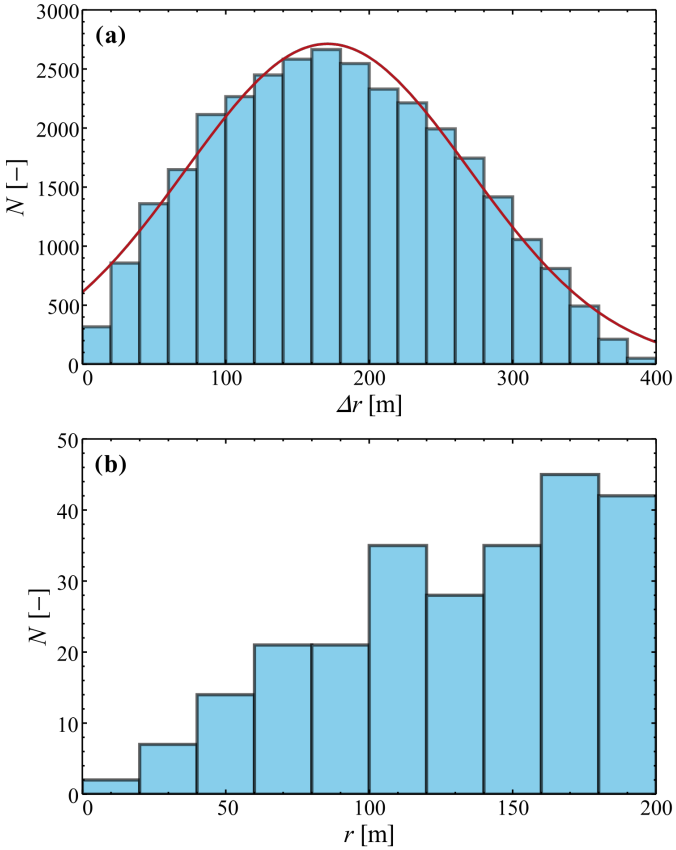

Fig. 2: For a system of $N = 250$ balls, *(a)* a histogram of the separation at equilibrium between each pair of balls produces an approximate Gaussian (red line) and *(b)* a histogram of the distance of each ball from the centre of the container at equilibrium shows that balls are more likely to be distributed away from the centre.

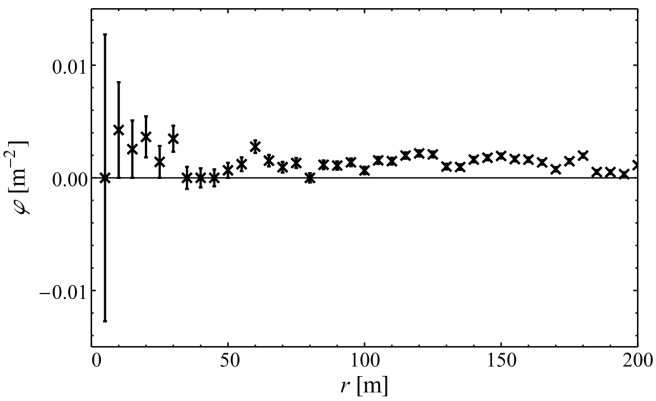

Fig. 3: At equilibrium, the concentration of the balls throughout the container is constant, so the concentration gradient is zero. For a circular container, this means balls are more likely to be distributed away from the centre (Fig. 2(b)).

($\bar{v}^2$) velocity of the system [3]. Increasing the temperature has skewed the graph towards the right as expected and the full-width at half-maximum (Δv) has increased from

$\Delta v = (11 \pm 1)\,\mathrm{m\,s^{-1}}$ to $\Delta v = (113 \pm 6)\,\mathrm{m\,s^{-1}}$.

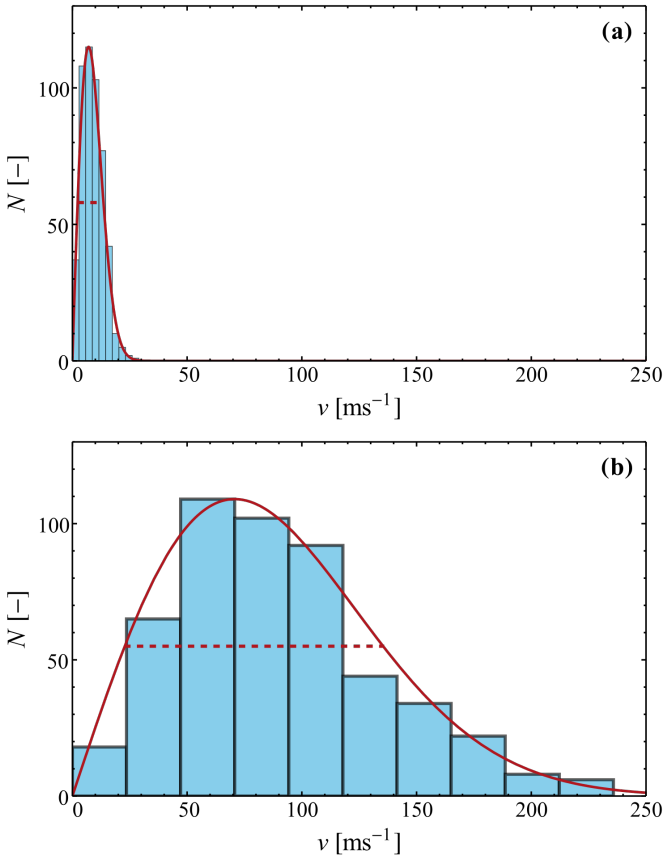

Fig. 4: A histogram of the velocity distribution at *(a)* low temperature ($\bar{v} = 10\,\mathrm{m\,s^{-1}}$) and *(b)* high temperature ($\bar{v} = 50\,\mathrm{m\,s^{-1}}$). The red lines show an approximate Rayleigh distribution. The Rayleigh parameter and COD, $[b^2, R^2]$, for *(a)* and *(b)* are $[(50 \pm 6)\,\mathrm{J\,kg^{-1}}, 0.98]$ and $[(5.0 \pm 0.6) \times 10^3\,\mathrm{J\,kg^{-1}}, 0.91]$, respectively. An increase in temperature reduces the peak height, increases the full-width at half-maximum (represented by dashed lines) and shifts the peak of the graph to the right.

B. Pressure Dependence on Macroscopic Properties

The pressure exerted on a 2D container is the impulse imparted per unit time on the circumference. The simulation is modified such that the initial position of each ball is randomly distributed and the initial velocity is selected from a Rayleigh distribution, mimicking equilibrium at $t = 0$. Pressure is the magnitude of impulse on the container divided by the total simulation time. By imposing that the system is in equilibrium at $t = 0$, we do not need to wait for the system to reach equilibrium so the uncertainty in the pressure is reduced. The error in the pressure is the standard deviation of the observed pressure after each B2W collision. For the following investigations, the number of balls is $N = 250$, the container radius is $R = 200\,\mathrm{m}$ and the RMS velocity is $\bar{v} = 50\,\mathrm{m\,s^{-1}}$ unless otherwise specified. Each simulation runs until 1250 B2B collisions have been observed.

First, we investigate the pressure dependence on temperature. The RMS velocity is varied from $\bar{v} = 10\,\mathrm{m\,s^{-1}}$ to $\bar{v} = 200\,\mathrm{m\,s^{-1}}$. A plot of pressure against $\bar{v}^2$ represents the pressure dependence on temperature as shown in Fig. 5. The plot is indicative of a strong linear correlation between pressure and temperature with a Pearson correlation coefficient (PCC) of $r = 0.9997$. This agrees with the ideal gas equation

$$p = \frac{Nk}{V}T. \tag{8}$$

We consider the pressure dependence on the radius of the container. The radius is varied from $R = 200\,\mathrm{m}$ to $R = 1000\,\mathrm{m}$. A plot of pressure against R^{-2} is shown in Fig. 6. There is a very strong linear correlation which is supported by a PCC value of $r = 0.999\,995$ indicating an almost-perfect linear correlation. The pressure dependence on container radius can be found by considering (8) in 2D, where the container volume term reduces to an area term which is proportional to R^2 for a circular container.

Lastly, we investigate the pressure dependence on number of balls in the container. The number of balls is varied from $N = 50$ to $N = 250$. A plot of pressure against N is shown in Fig. 7. The strong correlation is supported by a PCC value of $r = 0.9999$, which is indicative of a linear pressure dependence on N, as expected from (8).

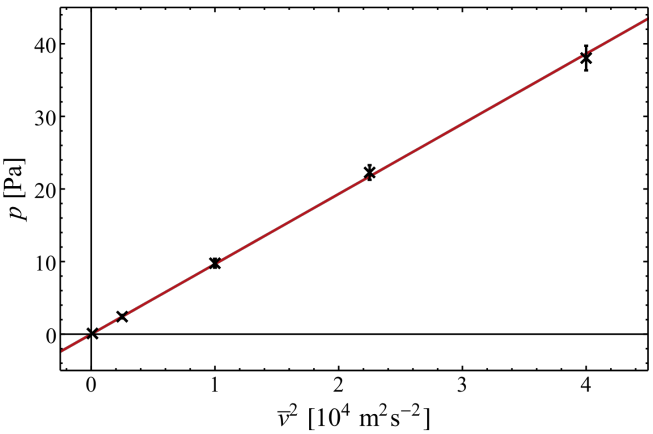

Fig. 5: A plot of the pressure exerted on the container when the RMS velocity is $\bar{v}$. The strong linear correlation is supported by a PCC value of $r = 0.997$, indicating $p \propto \bar{v}^2 \propto T$.

C. Van der Waals' Equation

We now investigate behaviour which deviates from that predicted by ideal gas theory. For balls of a finite radius, the modified Van der Waals equation of state is

$$p = \frac{NkT}{V - Nb}, \tag{9}$$

where we neglect the molecular interaction term. Expanding the Taylor series about $b = 0$ gives

$$p = \frac{NkT}{V}\left[1 + \frac{N}{V}b + O(b^2)\right]. \tag{10}$$

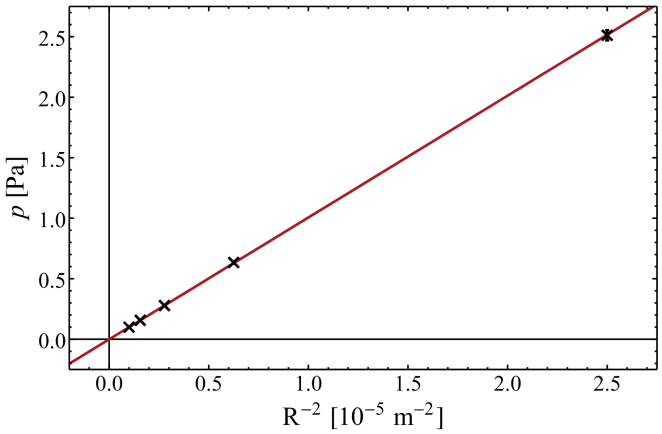

Fig. 6: A plot showing how the pressure varies with inverse square of the container radius. A PCC value of $r = 0.999\,995$ is indicative of a strongly linear correlation between p and R^{-2}.

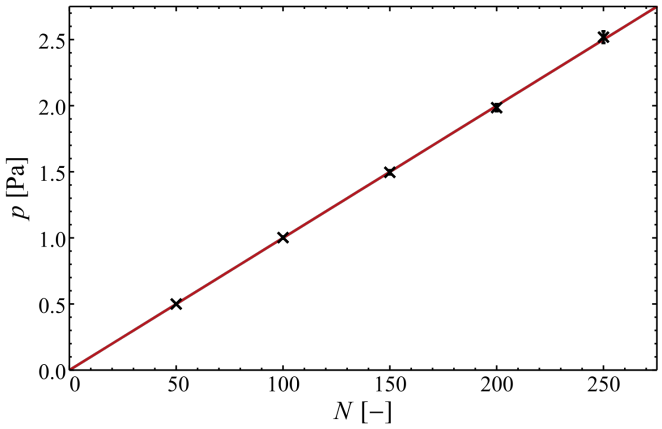

Fig. 7: A plot showing how the pressure exerted on the container is dependent on the number of balls in the container. This plot has PCC $r = 0.9999$ so the simulation results suggest $p \propto N$.

We expect $b \propto a^2$ since Nb represents the area excluded from the container due to finite ball radius, a. A plot of p against a in Fig. 8 shows the proposed relationship holds with the coefficient of the a^2 term equal to $(8.5 \pm 0.4)\,\mathrm{Pa\,m^{-2}}$. Even to a first order approximation, (10) strongly correlates with the simulation data and has a high goodness-of-fit with COD $R^2 = 0.992$.

Since (9) holds for this simulation, we aim to find b. The initial state is configured with container radius $R = 250\,\mathrm{m}$ and ball radius $a = 12\,\mathrm{m}$ is chosen so that a/R is not negligible. The number of balls is varied from $N = 5$ to $N = 200$ and pressure is calculated for each trial. A plot of pressure against N is shown in Fig. 9. A curve-fitting algorithm gives $V = (26 \pm 5) \times 10^3\,\mathrm{m^2}$ and $b = (90 \pm 20)\,\mathrm{m^2}$. The ratio of area excluded by each ball to the total container area is $b/V = (3.5 \pm 1.3) \times 10^{-3}$ and $\pi a^2/\pi R^2 = 2.3 \times 10^{-3}$, so b represents the expected quantity of area excluded by each ball.

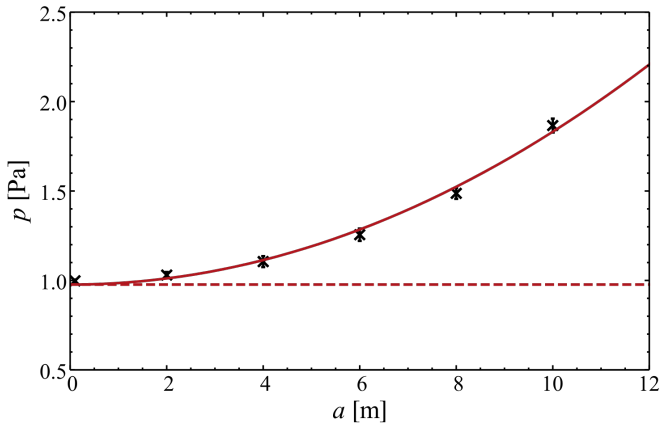

Fig. 8: A plot of the pressure exerted on the container against the ball radius. The dashed line represents the pressure dependence predicted by ideal gas theory, which deviates from the result for real gases with large a. This plot has COD $R^2 = 0.992$, suggesting strong goodness-of-fit.

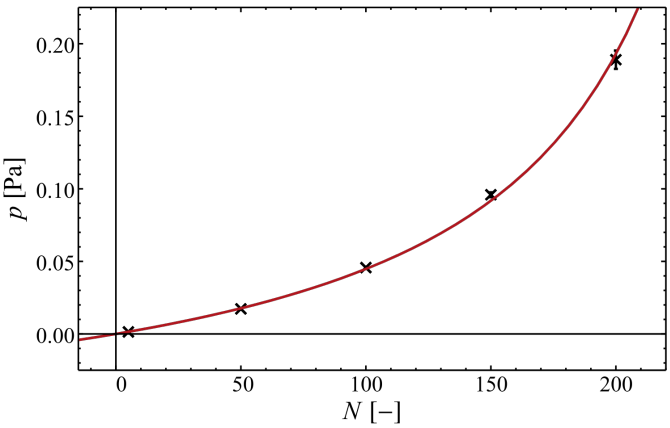

Fig. 9: A plot of the pressure exerted on the container by N balls each of which have finite radius $a = 12\,\mathrm{m}$. From (9), we obtain $b = (90 \pm 20)\,\mathrm{m^2}$ and $V = (26 \pm 5) \times 10^3\,\mathrm{m^2}$. The ratio b/V is approximately equal to the ratio $\pi a^2/\pi R^2$ where R is the radius of the container.

D. Mean Free Path

The mean free path (MFP), λ, is defined as the distance travelled by a particle per collision. From thermodynamics, λ satisfies [4]

$$\lambda = \frac{1}{\sqrt{2}\pi n d^2}, \tag{11}$$

where n is the number density and d is the diameter of each particle. For a rigid container, the number density is proportional to the number of particles, N, so we expect $\lambda \propto 1/N$.

In our simulation, MFP is the total distance travelled divided by the number of B2B collisions for each particle. The

simulation is configured with $\bar{v} = 10\,\mathrm{m\,s^{-1}}$ and the container radius is set to $R = 150\,\mathrm{m}$ to limit the MFP for small N. The number of balls is varied from $N = 50$ to $N = 650$ and a plot of λ^{-1} against N is produced (Fig. 10). The PCC value for this plot is $r = 0.998$ which indicates that the MFP is proportional to $1/N$ as expected.

The large error in λ^{-1} in Fig. 10 arises due to the spread in the MFP for balls in the container, giving uncertainties as large as $69.7\,\%$. This is caused by a systematic error whereby balls generated at the edge of the container may bounce along the walls of the container without many B2B collisions, giving disproportionately high MFPs. The error can be mitigated by changing the shape of the container, so that balls are unable to deflect along the edge of the container. Despite the large error, the means of the MFPs are strongly linearly correlated with $1/N$.

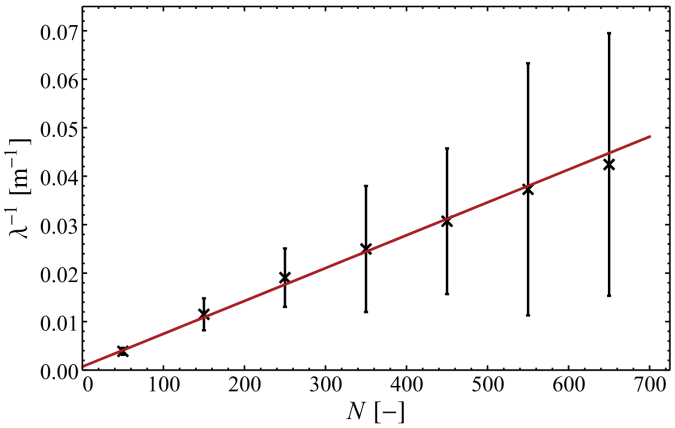

Fig. 10: A plot of the reciprocal mean free path of a particle against the number of particles in the container. The plot indicates a strong linear correlation with PCC value $r = 0.998$ suggesting $\lambda \propto 1/N$.

E. Diffusion Equation

We aim to investigate the diffusion coefficient dependence on the temperature. The initial state is configured such that $N = 450$ balls are concentrated in a circle of radius $r = 50\,\mathrm{m}$ within a container of radius $R = 350\,\mathrm{m}$ (Fig. 11). The diffusion equation expresses how the concentration, φ, of a substance varies with time [5]. In two-dimensional polar coordinates, the diffusion equation is

$$\frac{\partial \varphi}{\partial t} = D\left[\frac{\partial^2 \varphi}{\partial r^2} + \frac{1}{r}\frac{\partial \varphi}{\partial r} + \frac{1}{r^2}\frac{\partial^2 \varphi}{\partial \theta^2}\right], \tag{12}$$

where D is the diffusion coefficient, r is the radial distance and θ is the azimuthal angle. The system has radial symmetry at $t = 0$, so the last term can be neglected. A plot of concentration against radius (Fig. 12) indicates that $\varphi(r)$ is approximately linear for $45 < r < 55$ at $t = 0$ so the first term can also be neglected. The diffusion equation reduces to

$$\left.\frac{\partial \varphi}{\partial t}\right|_{t=0} = \left.\frac{D}{r}\frac{\partial \varphi}{\partial r}\right|_{45<r<55}. \tag{13}$$

A plot of concentration of the inner circle against time for $\bar{v} = 10\,\mathrm{m\,s^{-1}}$ is shown in Fig. 13, where the dashed line represents the initial rate of change of concentration.

The RMS velocity of the particles is varied from $\bar{v} = 10\,\mathrm{m\,s^{-1}}$ to $\bar{v} = 250\,\mathrm{m\,s^{-1}}$. For each trial, the initial rate of change of concentration and concentration gradient at $r = 50\,\mathrm{m}$ is calculated to determine the diffusion coefficient. A plot of the diffusion coefficient against $\bar{v}$ is shown in Fig. 14. A strong linear correlation exists with PCC value $r = 0.999$, suggesting that $D \propto \bar{v}$ so

$$D \propto \sqrt{T}, \tag{14}$$

for this two-dimensional simulation.

The largest source of error in this approximation is in the calculation of the concentration gradient, which is linearly interpolated between $r = 45\,\mathrm{m}$ and $r = 55\,\mathrm{m}$ giving uncertainties as high as $29.9\,\%$. Nevertheless, Fig. 14 shows that, despite the large error, there is a clear linear correlation between D and $\bar{v}$.

The concentration against time in Fig. 13 oscillates about the equilibrium with troughs at $t \approx 30\,\mathrm{s}, 52\,\mathrm{s}, 67\,\mathrm{s}$ and peaks at $t \approx 42\,\mathrm{s}, 62\,\mathrm{s}$. The oscillatory behaviour arises because the net divergence of the inner circle at $t = 0\,\mathrm{s}$ is positive but, once the balls have collided with the circular container, they are deflected back to the inner circle. Therefore, the net divergence is negative at $t \approx 42\,\mathrm{s}, 62\,\mathrm{s}$ so the concentration undergoes oscillation as the deflected balls pass through the inner circle. The oscillation reduces in amplitude with time as B2B collisions cause balls to deflect away from the inner circle. For $t > 70\,\mathrm{s}$, the oscillation is superseded by statistical noise.

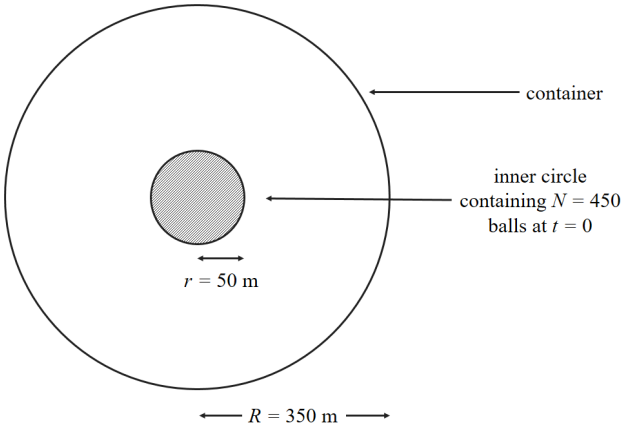

Fig. 11: The setup of the diffusion coefficient experiment. At $t = 0$, all $N = 450$ balls are generated in an inner circle of radius $r = 50\,\mathrm{m}$ within a container of radius $R = 350\,\mathrm{m}$.

V. Discussion & Improvements

A perpetual source of error with computer simulations is floating point arithmetic (FPA), which can cause imprecise rounding of decimal numbers. This leads to a fundamental flaw in the simulation when recalculating collision times, as one of

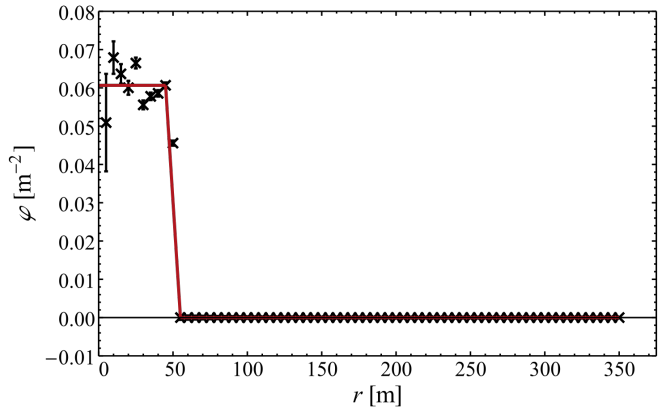

Fig. 12: A plot of the initial concentration gradient, where all of the balls are confined to a small circle within the container. The red line is an approximate representation of $\varphi(r)$ with linear interpolation applied between $r = 45\,\mathrm{m}$ and $r = 55\,\mathrm{m}$.

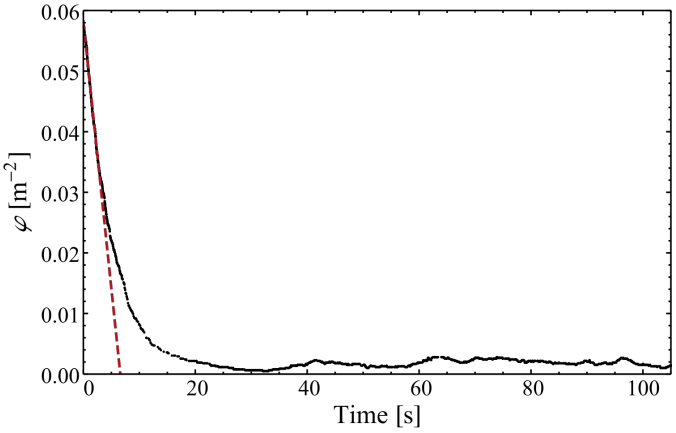

Fig. 13: A plot of concentration of the inner circle against time for a system with RMS velocity $\bar{v} = 10\,\mathrm{m\,s^{-1}}$ shows an exponential decay to an equilibrium concentration. The dashed line indicates the rate of change of concentration, $\partial\varphi/\partial t$, at $t = 0$. The experiment is repeated for varying values of $\bar{v}$ and $(\partial\varphi/\partial t)_{t=0}$ is calculated for each trial.

the roots of the quadratic will usually be zero immediately after a collision. FPA errors can result in the zero root being rounded to a small positive number of the order $t = 0.1\,\mathrm{ps}$, so the simulation assumes this is the time of the next collision. Neglecting roots with $t < 1\,\mathrm{ps}$ prevents this error arising, but introduces an error if a legitimate collision is due to occur within the next $1\,\mathrm{ps}$. By considering the mean free time, τ, for our system, we deduce that $\tau \gg 1\,\mathrm{ps}$ so the probability of this is negligibly small for our small-scale simulation. Hence, roots with $t < 1\,\mathrm{ps}$ can be justifiably neglected.

A natural extension to the simulation would be to model a three-dimensional container to reproduce a Maxwell-Boltzmann distribution and consider how (14) changes with the introduction of an additional degree of freedom. It would also be interesting to repeat the diffusion coefficient investigation with varying number density and ball radius to derive

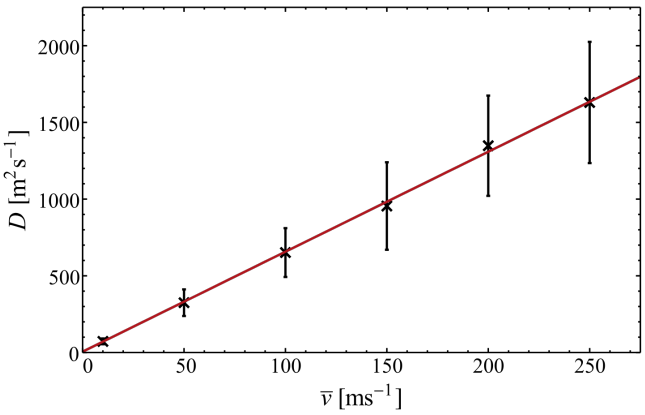

Fig. 14: A plot of the diffusion coefficient as a function of RMS velocity. The PCC value for this plot is $r = 0.999$ indicating $D \propto \bar{v}$. By extension, $D \propto \sqrt{T}$.

a complete expression for the functional form of the diffusion coefficient of real gases in terms of known thermodynamic variables.

VI. Conclusion

In this report, we have used a simple two-dimensional simulation of hard balls to recreate and verify the results of kinetic gas theory. The simulation was shown to corroborate the predictions of the ideal gas and Van der Waals equations of state. An investigation was conducted to verify the inverse proportionality relation between the mean free path and the particle number. The law of diffusion was investigated and a proportionality relation was found between the diffusion coefficient and the square root of the equilibrium temperature.

References

[1] J. M. Haile, Molecular Dynamics Simulation: Elementary Methods, New York: John Wiley Sons, Inc, 1992.
[2] J. Novak and A. B. Bortz, The Evolution of the Two-Dimensional Maxwell-Boltzmann Distribution, *American Journal of Physics*, vol. 38, no. 12, pp. 1402-1406, 1970.
[3] I. Grattan-Guinness, Landmark Writings in Western Mathematics 1640-1940, Amsterdam: Elsevier B.V., 2005.
[4] G. A. Bird, Definition of mean free path for real gases, *The Physics of Fluids*, vol. 26, no. 11, pp. 3222-3223, 1983.
[5] F. Adolf, Ueber diffusion, *Annalen der Physik*, vol. 170, no. 1, pp. 59-86, 1855.

APPENDIX A
CONSERVATION OF KINETIC ENERGY

The conservation of kinetic energy in the simulation is shown in Fig. 15. The analysis of this plot is not central to the report so it is included in the appendix for completeness of simulation testing.

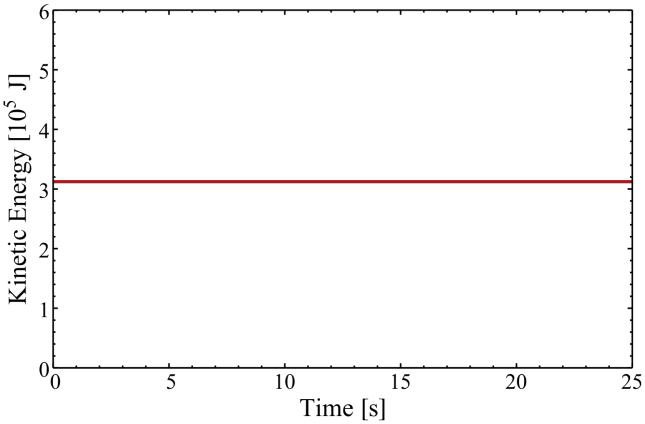

Fig. 15: A plot of the total kinetic energy of the system against time. The straight line indicates that kinetic energy and hence total energy is conserved in this simulation. The plot for the total magnitude of momentum is similar.